Journal of
Applied Crystallography

ISSN 0021-8898

Received 26 May 2011
Accepted 6 October 2011

A method to identify dislocations in a known crystal structure by transmission electron microscopy

Yudong Zhang,[a]* Shiying Wang,[a,b] Claude Esling,[a]* Jean-Sébastien Lecomte,[a] Christophe Schuman,[a] Xiang Zhao[b] and Liang Zuo[b]

[a]Laboratoire d'Étude des Microstructures et de Mécanique des Matériaux, LEM3 CNRS, (former LETAM, CNRS FRE 3143), University of Metz, 57045 Metz, France, and [b]Key Laboratory for Anisotropy and Texture of Materials (Ministry of Education), Northeastern University, Shenyang 110004, People's Republic of China. Correspondence e-mail: yudong.zhang@univ-metz.fr, claude.esling@univ-metz.fr

This paper proposes a method to identify the type and the Burgers vector of dislocations visualized *via* transmission electron microscopy (TEM). The first step is to determine experimentally the orientation, with respect to the sample holder, of a grain of known crystal structure whose dislocation slip systems have been previously reported. With this determined orientation of the grain, the method calculates the orientation of the projections of the possible dislocation line vectors in the transmission electron microscope screen coordinate system and then compares them with the observed dislocations to identify their type and the Burgers vector. The coordinate transformations underlying the method are outlined, and its validity is demonstrated using TEM measurements on a titanium sample. The method is expected to simplify the related TEM determination work.

1. Introduction

Various physical and metallurgical processes, such as plastic deformation, solid-state phase transformations and recrystallization, are characterized by dislocation activity. Identification of individual dislocations [dislocation type (edge, screw or mixed) and Burgers vector] appears to be particularly important to reveal the physical principles on which they are based. The identification of dislocations has been an important topic in the field of characterization by transmission electron microscopy (TEM). The classical determination technique is based on the '$\mathbf{g}\cdot\mathbf{b}$' invisibility criterion (Edington, 1975). The image of a dislocation becomes invisible when it lies in the reflecting plane. The scalar product of the diffraction vector, $\mathbf{g}$, and the Burgers vector, $\mathbf{b}$, is then zero. In this context, the Burgers vector of the dislocation could be uniquely determined with two independent tilt positions where the $\mathbf{g}\cdot\mathbf{b}=0$ condition is fulfilled. As $\mathbf{b}$ is common to these two independent reflections, $\mathbf{b}$ must be the zone axis of the two planes. Thus the Burgers vector is determined. In reality, the availability of $\mathbf{g}\cdot\mathbf{b}=0$ invisibility is limited, depending on the elastic anisotropy of the material. If the crystal is elastically anisotropic, significant contrast can occur when $\mathbf{g}\cdot\mathbf{b}=0$, increasing the ambiguities of practical determination. In this context, the computer aided image matching technique was developed (Head, 1967; Humble, 1968, 1970; Head *et al.*, 1973). The roughly determined Burgers vector $\mathbf{b}$ of the dislocation is further confirmed by matching the contrast of the observed dislocation image with that simulated. A detailed description of the computer image simulation procedure has been recently given by De Graef (2003). However, this technique cannot completely exclude the classical $\mathbf{g}\cdot\mathbf{b}=0$ determination procedure. It is rather based on this procedure, using it to obtain the initial input. The manipulation to obtain the invisibility condition is critical and requires great care and specialist experience. In many cases, no conclusions can be drawn after a long examination. In view of the difficulty, efforts have been made to ease the identification process with the TEM crystallographic orientation determination technique (Schwarzer, 1997; Schwarzer & Zaefferer, 1995; Morawiec, 1999; Morawiec *et al.*, 2002), which is similar to that used for scanning electron microscopy/electron backscatter diffraction. One representative study was carried out by Schwarzer & Zaefferer (1995). With the aid of TEM crystallographic orientation determination software (Schwarzer & Zaefferer, 1995; Morawiec *et al.*, 2002), the favorable $\mathbf{g}\cdot\mathbf{b}=0$ sample tilt position can be simulated instead of having to find the sample tilt directly, which sometimes involves blind searching. This technique significantly simplifies the determination process. However, the non-available invisibility situation still exists when the local orientation is not favorable or the material is strongly elastically anisotropic (Edington, 1975). Further efforts to simplify the determination technique are still necessary and possible.

After so many years of intensive study of dislocation slips in a wide range of materials, the dislocation slip systems (Burgers vector and slip plane) in many crystal structures are well known and well documented. If the crystallographic orientation of a grain of a known crystal structure is given, the

orientation of the dislocation lines in the crystal, and hence their projections on the transmission electron microscope screen under well defined sample loading, are uniquely defined. Examining the projections of all possible dislocations, the observed ones can be identified. From such a consideration, a method to identify pure screw or edge dislocations is proposed and demonstrated in this work. This method can be used as a countercheck to the classical $\mathbf{g} \cdot \mathbf{b} = 0$ invisibility determination technique. The proposed method is expected to significantly reduce the required examination work and facilitate related studies.

2. Methodology

The basic principle of the method is to calculate the possible dislocation line vectors in the transmission electron microscope screen coordinate system, using the determined crystallographic orientation of a grain with respect to the sample holder and the orientation of the sample holder with respect to the screen coordinate system. Then the projection of these line vectors on the screen is compared with the observed dislocation lines to identify the type and the Burgers vector of the dislocations observed. The complete method will be detailed in the following sections.

2.1. Setting of coordinate systems

Considering the characteristics of TEM for sample loading and imaging, it is convenient to introduce three Cartesian coordinate systems in addition to the crystal lattice basis. All the coordinate systems are of the same handedness, and they are orthonormal. In the present work, we choose the right-hand set. Of the three Cartesian coordinate systems, one is set to the screen of the transmission electron microscope that records the image of the dislocations. Its Z axis is set in the inverse direction of the incident electron beam. One coordinate system is set to the sample holder, also with its Z axis in the inverse direction of the incident electron beam when the holder is in the non-tilted position. The third is set to the crystal. The setting of this coordinate system is not fixed but variable. It can follow the convention used by the software *Channel 5* (Oxford Diffraction, 2006), for example. The orientation relationships between the Cartesian coordinate systems are defined with a triplet of rotations (Euler angles in Bunge notation; Bunge *et al.*, 1981), transforming one coordinate system into the other. It should be noted that the setting of the coordinate systems is not unique. There are several ways to define the corresponding reference frames, depending on the sample loading manner of the microscope and the targeted work. A complete and pedagogic description of the choice of the reference systems from the examined defect in the crystal to the screen of the transmission electron microscope and the corresponding coordinate transformation matrices is given by De Graef (2003).

2.2. Determination of the dislocation line vector in the crystal lattice basis

As in TEM only dislocation lines are visible, the dislocation type and Burgers vector can be identified by examining the projection of the dislocation lines. For a given dislocation slip system in a known crystal system, the dislocation type (pure screw or pure edge) and its Burgers vector are defined. For screw dislocations, as the dislocation line is parallel to its Burgers vector by definition, the line vector can be taken as the Burgers vector. This means that the coordinates of the dislocation line in the crystal basis (*i.e.* in the Bravais lattice) can be expressed by the Miller indices. For edge dislocations, as the dislocation line lies in the slip plane and is perpendicular to the Burgers vector, the line vector in the crystal basis can be obtained by the cross product of the slip plane normal and the corresponding Burgers vector. Before entering into the calculation procedure in detail, let us briefly review the corresponding fundamental properties concerning the direct and reciprocal space of a crystal lattice. First, a lattice plane in direct space with Miller indices (*hkl*) corresponds to a lattice vector that is normal to this plane with the same indices as coordinates in reciprocal space and *vice versa*. Second, the vector product of two lattice vectors in direct space results in a vector with the corresponding coordinates in reciprocal space and *vice versa*. Third, the coordinate transformation between the two spaces can be easily performed using the corresponding direct and reciprocal metric tensors (Shmueli, 1996). Now we come to the calculation procedure of the edge dislocation line vector. With the direct metric tensor, the components of the Burgers vector in reciprocal space can be calculated as follows:

$$\begin{pmatrix} u^* \\ v^* \\ w^* \end{pmatrix} = G \begin{pmatrix} u \\ v \\ w \end{pmatrix}, \tag{1}$$

where u, v and w are the Miller indices of the Burgers vector; u^*, v^* and w^* are the components of the Burgers vector in reciprocal space; and G is the metric tensor of direct space (Shmueli, 1996). Therefore, the proportional coordinates of the vector indicating the direction of the dislocation line in the crystal basis can be obtained by the vector cross product of the slip plane normal vector and the covariant Burgers vector in reciprocal space:

$$\begin{pmatrix} kw^* - lv^* \\ lu^* - kw^* \\ hv^* - ku^* \end{pmatrix}, \tag{2}$$

where h, k and l are the Miller indices of the slip plane.

2.3. Coordinate transformation from the screen coordinate system to the crystal basis

The coordinate transformation from the screen coordinate system to the crystal basis can be decomposed into the following two or three steps depending on the crystal basis: the transformation from the screen coordinate system to the sample holder coordinate system, the transformation from the sample holder coordinate system to the Cartesian coordinate system linked to the crystal lattice basis and the transformation from this Cartesian coordinate system to the possibly non-Cartesian crystal basis.

Table 1
Summary of the two-step (R_1 and R_2) coordinate transformations from the screen coordinate system to the final tilted sample holder positions.

The coordinate transformations are parametrized by a triplet of rotations expressed in Euler angles.

	R_2		
R_1	α tilt (°)	β tilt (°)	γ tilt (°)
(φ_M, 0, 0)	(0, α, 0)	(90, β, −90)	(γ, 0, 0)

The transformation from the screen coordinate system to the sample holder coordinate system depends on the individual operation that includes the magnetic rotation (if not corrected by the transmission electron microscope) and the tilt of the sample holder. The transformation can be further decomposed into two steps, R_1 and R_2, given that the magnification-dependent magnetic rotation is not corrected by the microscope. As the two coordinate systems are orthonormal, each transformation can be parameterized by a triplet of rotations [Euler angles (φ_1, Φ, φ_2) in Bunge's notation (Bunge *et al.*, 1981)]. The first step is from the screen system to the non-tilted sample holder system (this is characterized by the calibrated magnification-dependent magnetic rotation, φ_M, around the Z axis of the screen coordinate system). The second step is from the non-tilted to the final tilted sample holder position. According to the characteristics of the commercially available TEM sample holders, there are two kinds of tilt combinations: α tilt (around the X axis of the sample holder) + β tilt (around the Y axis of the sample holder) and α tilt + γ rotation (around the Z axis of the sample holder). All these rotations in their Euler angle representation are summarized in Table 1. With the rotations described, the transformation matrix can be built as follows (in matrix notation):

$$M_{s\rightarrow h} = M_{R_1} M_{R_2}, \qquad (3)$$

where $M_{s\rightarrow h}$ is the coordinate transformation matrix from the screen coordinate system to the final tilted sample holder position, M_{R_1} the transformation from the screen coordinate system to the non-tilted sample holder position and M_{R_2} the transformation from the non-tilted to the final tilted sample holder position. Special attention should be paid to the sequence of the combined tilt operations during the TEM examination. The multiplication sequence of the submatrices of M_{R_2} should conform to the corresponding tilt sequence.

The coordinate transformation from the final sample holder position to the Cartesian crystal reference frame can be performed on the basis of the experimentally determined orientation of the crystal with respect to the sample holder. The orientation of the crystal can be directly determined, for example, by indexing the Kikuchi line pattern using the software *Euclid Phantasies* (*EP*; Morawiec, 1999; Morawiec *et al.*, 2002). Then, three Euler angles of the rotations transforming the sample holder coordinate system to the Cartesian crystal reference linked to the crystal lattice basis are given by the software. Thus the corresponding transformation matrix, $M_{h\rightarrow CarCry}$, can be constructed.

The orientation relationship between the Cartesian crystal coordinate system and the not necessarily orthonormal Bravais lattice basis is set under the convention given by *Channel 5* (Oxford Diffraction, 2006). Thus the transformation matrix $M_{CarCry\rightarrow BraLatt}$ is defined.

Then the transformation matrix $M_{s\rightarrow BraLatt}$ from the screen coordinate system to the crystal basis (Bravais lattice) can be obtained:

$$M_{s\rightarrow BraLatt} = M_{s\rightarrow h}\, M_{h\rightarrow CarCry}\, M_{CarCry\rightarrow BraLatt}. \qquad (4)$$

2.4. Identification of the dislocation system

Using equation (4), the dislocation line vector can be calculated in the screen coordinate system through coordinate transformation. The X- and Y-axis coordinates of the vector define its projection on the screen plane. In this way, the projections of all the possible dislocation lines for a given crystal structure can be calculated according to the crystal orientation. By comparing the possible lines (intersection angle of the projection with one of the two axes X or Y) with those of the actually observed dislocation lines, the type and the Burgers vector of the effective dislocation systems can be selected according to the best match criterion.

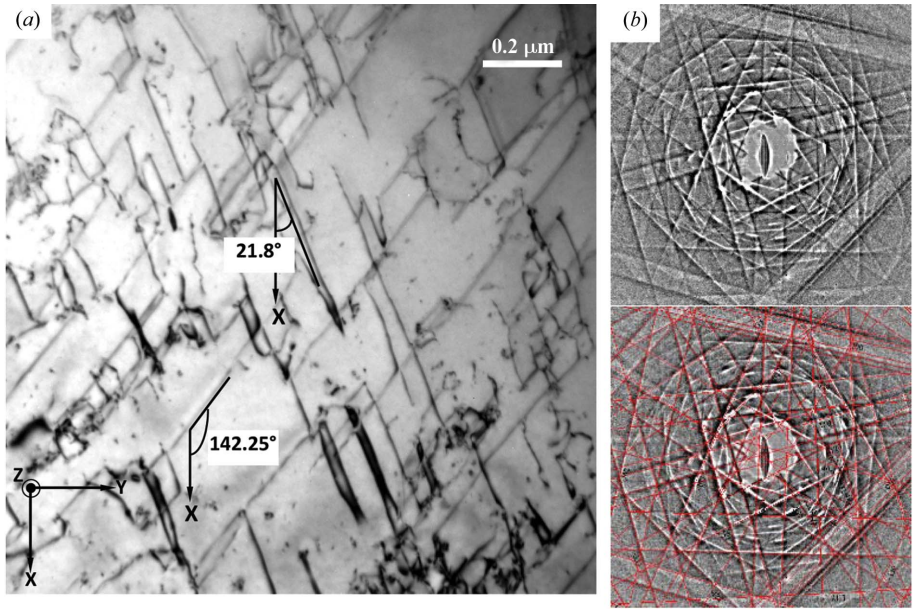

Figure 1
(*a*) Bright-field image of the interior of a deformed T40 grain and the screen coordinate system. (*b*) Kikuchi line pattern acquired from the same area (top) and the pattern overlapped with the pattern recalculated by *EP* (bottom).

Table 2
TEM magnetic rotations and sample holder tilt angles to acquire the bright-field image and the Kikuchi line pattern, and the determined orientation of the grain by *EP*.

Magnetic rotation (°)†		Sample holder tilt (°)		Orientation (°)‡		
Diffraction mode	Image mode	α tilt	β tilt	φ_1	Φ	φ_2
119.33	125.57	18.52	0	320.163	−20.437	234.388

† Magnetic rotation about the Z axis of the screen coordinate system. ‡ Euler angles in Bunge notation of the orientation determined by *EP*.

Table 3
Five well documented dislocation slip systems in titanium (Partridge, 1967; Yoo, 1981; Kelly *et al.*, 2000).

Name	System	
Basal slip	{0001}	$\langle 1\bar{2}10\rangle$
Prismatic	$\{10\bar{1}0\}$	$\langle \bar{1}2\bar{1}0\rangle$
Pyramidal $\langle a\rangle$	$\{10\bar{1}1\}$	$\langle \bar{1}2\bar{1}0\rangle$
Pyramidal $\langle a+c\rangle\pi_1$	$\{10\bar{1}1\}$	$\langle 2\bar{1}\bar{1}3\rangle$
Pyramidal $\langle a+c\rangle\pi_2$	$\{2\bar{1}\bar{1}2\}$	$\langle 2\bar{1}\bar{1}3\rangle$

3. Application example

In this section, we present an example to illustrate the application of the method. The material used in this example is commercially pure titanium T40. The plate sample with dimensions 30 × 18 × 1.6 mm was sheared by 5% at room temperature. The sample was then mechanically thinned to 100–150 µm in thickness. TEM 3 mm discs were electrolytically cut from the thinned plate in a solution of 10% perchloric acid in methanol at a voltage of 17 V and a temperature in the range from 258 to 263 K, using Struers TenuPol-5. The final thinning to render the discs transparent to electrons for TEM was performed in the same solution under the same conditions. The TEM examination was performed using a Philips CM200 equipped with the orientation determination software *EP*.

Fig. 1(*a*) shows a bright-field image of the interior of a deformed T40 grain, where two sets of differently oriented dislocation lines can be observed. The angles of the two types of dislocation lines with respect to the X axis of the screen coordinate system are measured to be 142.25 and 21.8°, respectively, as indicated in the figure. A Kikuchi line pattern acquired from the same area is displayed in Fig. 1(*b*). The pattern was indexed using *EP* and the Euler angles expressing the orientation of the grain (φ_1, Φ, φ_2) in Bunge notation with respect to the sample holder coordinate system are (320.163, −20.437, 234.388°). The pattern recalculated by *EP* (in red) matches well the measured pattern and is displayed below the raw pattern in Fig. 1(*b*). The TEM magnetic rotation angles in image and diffraction modes and the sample holder tilt angles at which the bright-field image and the diffraction pattern are acquired are given in Table 2. Five well identified dislocation slip systems in titanium reported in the literature (Partridge, 1967; Yoo, 1981; Kelly *et al.*, 2000) are shown in Table 3 as potential candidates. With the above experimental parameters and the grain orientation determined, the angles of the projection of the candidate dislocation lines with respect to the X axis of the screen coordinate system were calculated (Table 4). Comparing the angles measured for the dislocation lines observed with those calculated, one can conclude that screw dislocations with the Burgers vectors $[\bar{1}\bar{1}20]$ (22.2926°) and $[\bar{2}110]$ (142.863°) have the best fit with the respective measured angles, as highlighted in bold in Table 3. This indicates that the dislocation lines appearing in the deformed grain are two variants of screw $\langle a\rangle$ dislocations.

Table 4
Angles of the projection of the candidate dislocation lines with the X axis of the screen coordinate system calculated using the determined orientation of the grain and the identification method.

			Angle of projection (°)	
Name	System		Edge	Screw
Basal	(0001)	$[1\bar{2}10]$	172.917	81.5362
	(0001)	$[\bar{1}\bar{1}20]$	112.167	**22.2926**
	(0001)	$[\bar{2}110]$	51.6076	**142.863**
Prismatic	$(10\bar{1}0)$	$[1\bar{2}10]$	114.588	81.5362
	$(1\bar{1}00)$	$[\bar{1}\bar{1}20]$	114.588	**22.2926**
	$(0\bar{1}10)$	$[\bar{2}110]$	114.588	**142.863**
Pyramidal $\langle a\rangle$	$(1\bar{1}0\bar{1})$	$[11\bar{2}0]$	110.35	**22.2926**
	$(1\bar{1}01)$	$[\bar{1}\bar{1}20]$	112.894	**22.2926**
	$(10\bar{1}1)$	$[\bar{1}2\bar{1}0]$	17.6085	81.5362
	$(10\bar{1}1)$	$[1\bar{2}10]$	156.568	81.5362
	$(0\bar{1}1\bar{1})$	$[2\bar{1}\bar{1}0]$	26.7887	**142.863**
	$(0\bar{1}11)$	$[\bar{2}110]$	69.0528	**142.863**
Pyramidal $\langle a+c\rangle\pi_1$	$(01\bar{1}1)$	$[11\bar{2}3]$	136.38	2.68119
	$(\bar{1}01\bar{1})$	$[\bar{1}\bar{1}23]$	90.4966	2.68119
	$(0\bar{1}11)$	$[\bar{1}\bar{1}2\bar{3}]$	134.112	42.4349
	$(10\bar{1}1)$	$[11\bar{2}3]$	87.7354	42.4349
	$(0\bar{1}1\bar{1})$	$[1\bar{2}13]$	148.702	65.3134
	$(\bar{1}101)$	$[1\bar{2}1\bar{3}]$	18.0689	65.3134
	$(1\bar{1}01)$	$[1\bar{2}1\bar{3}]$	11.8758	90.2685
	$(01\bar{1}1)$	$[\bar{1}2\bar{1}3]$	152.458	90.2685
	$(10\bar{1}1)$	$[2\bar{1}\bar{1}3]$	71.766	135.343
	$(\bar{1}10\bar{1})$	$[\bar{2}113]$	32.7488	135.343
	$(1\bar{1}0\bar{1})$	$[2\bar{1}\bar{1}3]$	26.4953	157.4
	$(\bar{1}011)$	$[\bar{2}11\bar{3}]$	75.9286	157.4
Pyramidal $\langle a+c\rangle\pi_2$	$(2\bar{1}\bar{1}2)$	$[2\bar{1}13]$	51.6076	135.343
	$(2\bar{1}\bar{1}2)$	$[2\bar{1}13]$	51.6076	157.4
	$(\bar{1}\bar{1}22)$	$[\bar{1}\bar{1}2\bar{3}]$	112.167	42.4349
	$(\bar{1}\bar{1}2\bar{2})$	$[\bar{1}\bar{1}23]$	112.167	2.68119
	$(1\bar{2}12)$	$[1\bar{2}1\bar{3}]$	172.917	90.2685
	$(1\bar{2}1\bar{2})$	$[1\bar{2}13]$	172.917	65.3134

To check the validity of the method, the sample was further tilted about the X axis of the sample holder to α = 12.98 and −4.30° to obtain the invisibility criteria for the respective $[\bar{1}\bar{1}20]$ and $[\bar{2}110]$ dislocations. Fig. 2 shows the dark-field images obtained using the $(\bar{2}20\bar{1})$ reflection at α = 12.98° and the $(01\bar{1}\bar{1})$ reflection at α = −4.30°. It is seen that, from Fig. 2(*a*), the $[\bar{1}\bar{1}20]$ dislocations are invisible and the scalar product of the reflection vector and the Burgers vector $\mathbf{g}_{\bar{2}20\bar{1}} \cdot \mathbf{b}_{\bar{1}\bar{1}20}$ is zero, while from Fig. 2(*b*), the $[\bar{2}110]$ dislocations are invisible and the scalar product of the reflection vector and the Burgers vector $\mathbf{g}_{01\bar{1}\bar{1}} \cdot \mathbf{b}_{\bar{2}110}$ is zero. In both cases the $\mathbf{g} \cdot \mathbf{b} = 0$ conditions are satisfied. This demonstrates that the proposed method could correctly identify the type and the Burgers vectors of the dislocations observed.

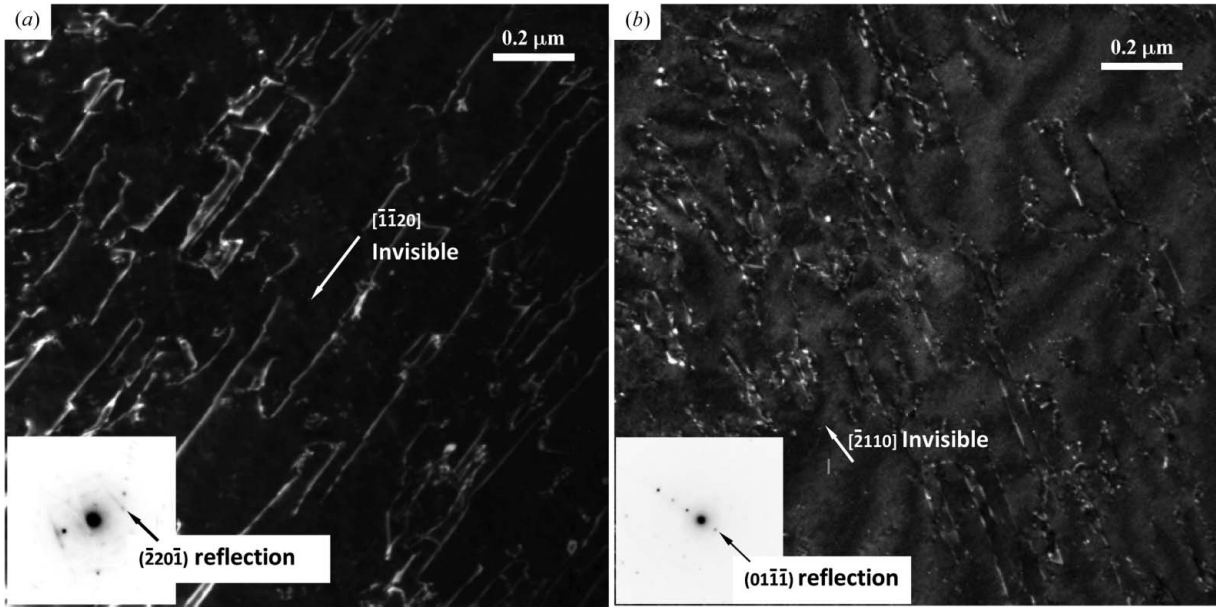

Figure 2
(*a*) Dark-field image using the $(\bar{2}20\bar{1})$ reflection at an α tilt angle of 12.98° where the $[\bar{1}\bar{1}20]$ dislocations are invisible. (*b*) Dark-field image using the $(01\bar{1}\bar{1})$ reflection at an α tilt angle of −4.30° where the $[\bar{2}110]$ dislocations are invisible.

4. Summary

In summary, a new method for identifying dislocations (type and Burgers vector) observed *via* TEM is proposed in this work. For a given crystal structure, the possible dislocation line projections on a transmission electron microscope screen are calculated using the determined crystallographic orientation of the crystal. Then the calculated projections are compared with those observed on the microscope screen to conclude the types and Burgers vectors of the dislocations observed. With this method, no special efforts in searching the $\mathbf{g} \cdot \mathbf{b} = 0$ invisibility conditions are required and the related examination work is dramatically simplified.

This work was supported by the Ministry of Education of China (under project No. B07015), by the CNRS (PICS No. 4164) and by the joint Chinese–French project OPTIMAG (grant No. ANR-09-BLAN-0382). The authors are grateful to Dr Jean-Jacques Fundenberger for the discussion about the software *Euclid's Phantasies* (*EP*).

References

Bunge, H. J., Esling, C. & Muller, J. (1981). *Acta Cryst.* A**37**, 889–899.
De Graef, M. (2003). *Introduction to Conventional Transmission Electron Microscopy*. Cambridge University Press.
Edington, J. W. (1975). *Practical Electron Microscopy in Materials Science*, Monograph 3, *Interpretation of Transmission Electron Micrographs*. Eindhoven: Philips Technical Library.
Head, A. K. (1967). *Aust. J. Phys.* **20**, 557–566.
Head, A. K., Humble, P., Glarebrough, L. M., Morton, A. J. & Forwood, C. T. (1973). *Computed Electron Micrographs and Defect Identification*. Amsterdam: North-Holland.
Humble, P. (1968). *Phys. Status Solidi*, **30**, 183–192.
Humble, P. (1970). *Diffraction and Imaging Techniques in Materials Science.* Amsterdam: North-Holland.
Kelly, A., Groves, G. W. & Kidd, P. (2000). *Crystallography and Crystal Defects*, revised ed. New York: John Wiley and Sons.
Morawiec, A. (1999). *J. Appl. Cryst.* **32**, 788–798.
Morawiec, A., Fundenberger, J.-J., Bouzy, E. & Lecomte, J.-S. (2002). *J. Appl. Cryst.* **35**, 287.
Oxford Diffraction (2006). *Channel 5*. Oxford Diffraction Ltd, Abingdon, Oxfordshire, UK.
Partridge, P. G. (1967). *Metall. Rev.* **12**, 169–194.
Schwarzer, R. A. (1997). *Ultramicroscopy*, **67**, 19–24.
Schwarzer, R. A. & Zaefferer, S. (1995). *Adv. X-ray Anal.* **38**, 377–381.
Shmueli, U. (1996). *International Tables for Crystallography*, Vol. B, *Reciprocal Space*, 1st ed. Dordrecht: Kluwer Academic Publishers.
Yoo, M. H. (1981). *Metall. Trans. A*, **12**, 409–418.